Interface

The well-tuned blues: the role of structural colours as optical signals in the species recognition of a local butterfly fauna (Lepidoptera: Lycaenidae: Polyommatinae)

Zsolt Bálint, Krisztián Kertész, Gábor Piszter, Zofia Vértesy and László P. Biró

Supplementary data	"Data Supplement" http://rsif.royalsocietypublishing.org/content/suppl/2012/02/01/rsif.2011.0854.DC1.html
References	**This article cites 42 articles, 7 of which can be accessed free** http://rsif.royalsocietypublishing.org/content/9/73/1745.full.html#ref-list-1
Email alerting service	Receive free email alerts when new articles cite this article - sign up in the box at the top right-hand corner of the article or click **here**

The well-tuned blues: the role of structural colours as optical signals in the species recognition of a local butterfly fauna (Lepidoptera: Lycaenidae: Polyommatinae)

Zsolt Bálint[1],*, Krisztián Kertész[2], Gábor Piszter[2], Zofia Vértesy[2] and László P. Biró[2]

[1]*Hungarian Natural History Museum, Baross utca 13, 1088 Budapest, Hungary*
[2]*Research Institute for Technical Physics and Materials Science, PO Box 49, 1525 Budapest, Hungary*

The photonic nanoarchitectures responsible for the blue colour of the males of nine polyommatine butterfly species living in the same site were investigated structurally by electron microscopy and spectrally by reflectance spectroscopy. Optical characterization was carried out on 110 exemplars. The structural data extracted by dedicated software and the spectral data extracted by standard software were inputted into an artificial neural network software to test the specificity of the structural and optical characteristics. It was found that both the structural and the spectral data allow species identification with an accuracy better than 90 per cent. The reflectance data were further analysed using a colour representation diagram built in a manner analogous to that of the human Commission Internationale de l'Eclairage diagram, but the additional blue visual pigment of lycaenid butterflies was taken into account. It was found that this butterfly-specific colour representation diagram yielded a much clearer distinction of the position of the investigated species compared with previous calculations using the human colour space. The specific colours of the investigated species were correlated with the 285 flight-period data points extracted from museum collections. The species with somewhat similar colours fly in distinct periods of the year such that the blue colours are well tuned for safe mate/competitor recognition. This allows for the creation of an effective pre-zygotic isolation mechanism for closely related synchronic and syntopic species.

Keywords: photonic nanoarchitecture; colour; butterfly scale; reflectance spectra; artificial neural network; flight period

1. INTRODUCTION

Polyommatine lycaenids, or blue butterflies, comprise an important portion of the Northern Hemisphere's Lepidoptera fauna. In open grassland habitats, they produce very high individual numbers. Entomologists working in the field with these butterflies and curators dealing with museum material identify individuals of different species mainly based on 'traditional' characteristics provided by the pattern displayed on ventral wing surfaces. However, this kind of approach to the identification of blue species may be regarded as anthropogenic because the practice is not based on precise knowledge of the way in which taxa discriminate themselves *in situ*.

*Author for correspondence (balint@nhmus.hu).

The males of many polyommatine lycaenids have blue arising from complex nanoarchitectures capable of interacting in a spectrally selective way with white light [1–4]. These photonic-crystal (PhC)-type nanoarchitectures are generated by intricate processes of self-assembly during scale formation in the pupal stage [5,6]. The advantages offered by producing these complex and specific nanoarchitectures must be important enough to support their formation and rigorous reproduction in subsequent generations. It has been demonstrated that they play an important role in the sexual communication of blues in potential mate and competitor recognition [7–9]. Indeed, the importance of male dorsal wing coloration in natural selection has been stressed by the role of coloration in pre-zygotic isolation mechanisms, such as reinforcement [10] and discoloration [11].

The PhC (regular structure) or photonic-band gap (PBG; quasi-ordered structure) materials [12,13] are composed of two non-absorbing media with refractive indexes that are sufficiently different (refractive index contrast) to create a PBG [14]. PhC or PBG materials with PBGs in the visible range in fact are nanocomposites. In butterfly scales, the nanocomposite is composed mainly of chitin and air [1,15]. As long as the refractive index contrast remains constant, the spectral position of the PBG is determined by the characteristic size and symmetry of the building elements constituting the nanoarchitecture, in a manner very similar to how the electronic band gaps of semiconductors are dependent on the crystal structure [14]. Practically, this means that to have a reflectivity spectrum characteristic for a certain species, the nanoarchitecture generating it must be species-specific and well preserved from generation to generation.

The often-colourful wings of butterflies are covered by scales with typical dimensions of approximately $100 \times 50 \times 1 \ \mu m^3$. Extensive studies have been published on butterfly wing coloration, which is frequently attributable only to pigments [16], a topic not discussed in our work. The photonic nanoarchitectures responsible for colour can be located in the volume of the scale—this is the case for the butterflies investigated in the present work—or in the ridges and cross-ribs. For a more-detailed presentation of scale structure and colour-generation mechanisms, see Biró & Vigneron [1].

Such nanocomposites as those occurring in butterfly scales have been a focus of attention for the physics and material science communities for only the last 20 years, since the production of the first 'yablonovite' structure [12]. This is despite the fact that biological evolution has produced and optimized such photonic nanoarchitectures for several hundreds of millennia [17]. A particularly rich variety of such structural colours is found in the insect world [1,18–21]. These photonic nanoarchitectures are attracting a growing scientific interest. The sources of this interest are numerous, ranging from the possibility of reproducing these nanoarchitectures to generate vivid colours from environmentally friendly materials to the extraction of new, bioinspired construction principles for synthetic PhC and PBG materials from naturally occurring photonic nanoarchitectures. A very attractive property of PBG-type materials concerns their ability to be used in displays operating in open air: the brightness of the colour increases with the increasing intensity of solar illumination, which is opposite to how most current displays operate. The first successful displays operating with PhCs were reported recently [22].

In a recent scatterometric study [4], it was shown that although they possess similar-looking photonic nanoarchitectures in their scales—as revealed by scanning electron microscopy (SEM)—several different lycaenid butterflies may exhibit different colours and very different scattering patterns. The authors underline in their paper that there is no simple relationship between the perforated layer structure of the scales and the scattering maps they obtained. Structures that appear similar in an SEM image may have different scattering maps (for instance, the perforation factors of the scales in figure 2h–j in Wilts *et al.* [4] are almost identical, but both the colour and the scattering diagrams differ). These findings underline that a more-

detailed study using cross-sectional transmission electron microscopy (TEM) to reveal the structure of the scales in a plane normal to the surface of the scales may provide additional insight into the relationship between structure, colour and scattering.

Regarding the biology of blue butterflies, a simple and at the same time conspicuous (long-range) signal may facilitate the finding of the right mate and the identification of potential competitors under natural conditions in flight and against a complex optical background. This signal must be clear and should be possible to detect and analyse in flight (see, for example, in the electronic supplementary material, the flashing signals emitted by the wings of a male Adonis blue (*Polyommatus bellargus*) in flight inside a cage: vid_1.avi). This signal is probably the 'long-range' opening accord for courtship, which is followed by olfactory (chemical) stimuli dissemination and the detection of scents (close range). The mating is closed by mechanical (physical) copula, when the transmission of genetic material takes place. We have already hypothesized that this pre-mating signal is optical in nature and have demonstrated, using museum samples, that the structural colours can be used for taxonomic discrimination [23,24]. Field observations also support the notion that the signals emitted by the surfaces of male wings communicate important information between individual butterflies in initiating successful courtships [7].

In this study, we investigated, both spectrally and structurally, the diverse colours of nine blue polyommatine butterfly species living in the same habitat, and we show that the hue of the blue sexual signal is tuned to the characteristic flying period of the various species. It may be hypothesized that the spectrally different colours, which arise from structurally characteristic nanoarchitectures, may be used by butterflies to generate long-range, species-specific recognition signals. To verify this assumption, we measured, under reproducible conditions, the reflectance spectra of more than 100 individuals of the nine species and used neural network software to discriminate between the species [25]. The species we selected live in the same habitat, i.e. under the same conditions of light and climate, and are closely related. Therefore, it is worth examining to what extent the nanoarchitectures responsible for the species-specific blue coloration of the males can be discriminated from one other by a similar neural network approach. Our earlier investigations [11,26–28] suggest that 'pepper-pot' photonic nanocomposites, typical for polyommatine blues [29], may be characteristic for each species, which is also suggested by the characteristic coloration of the wings observed by the naked eye (figure 1). In the case of the nine investigated species—all possessing different hues of blue—this could offer a starting point to better understand the biological rules that associate a certain nanoarchitecture with a certain colour (reflectance spectrum).

2. MATERIAL AND METHODS

2.1. Materials

We chose nine species representing the *Polyommatus* genus group in the family Lycaenidae. This composition
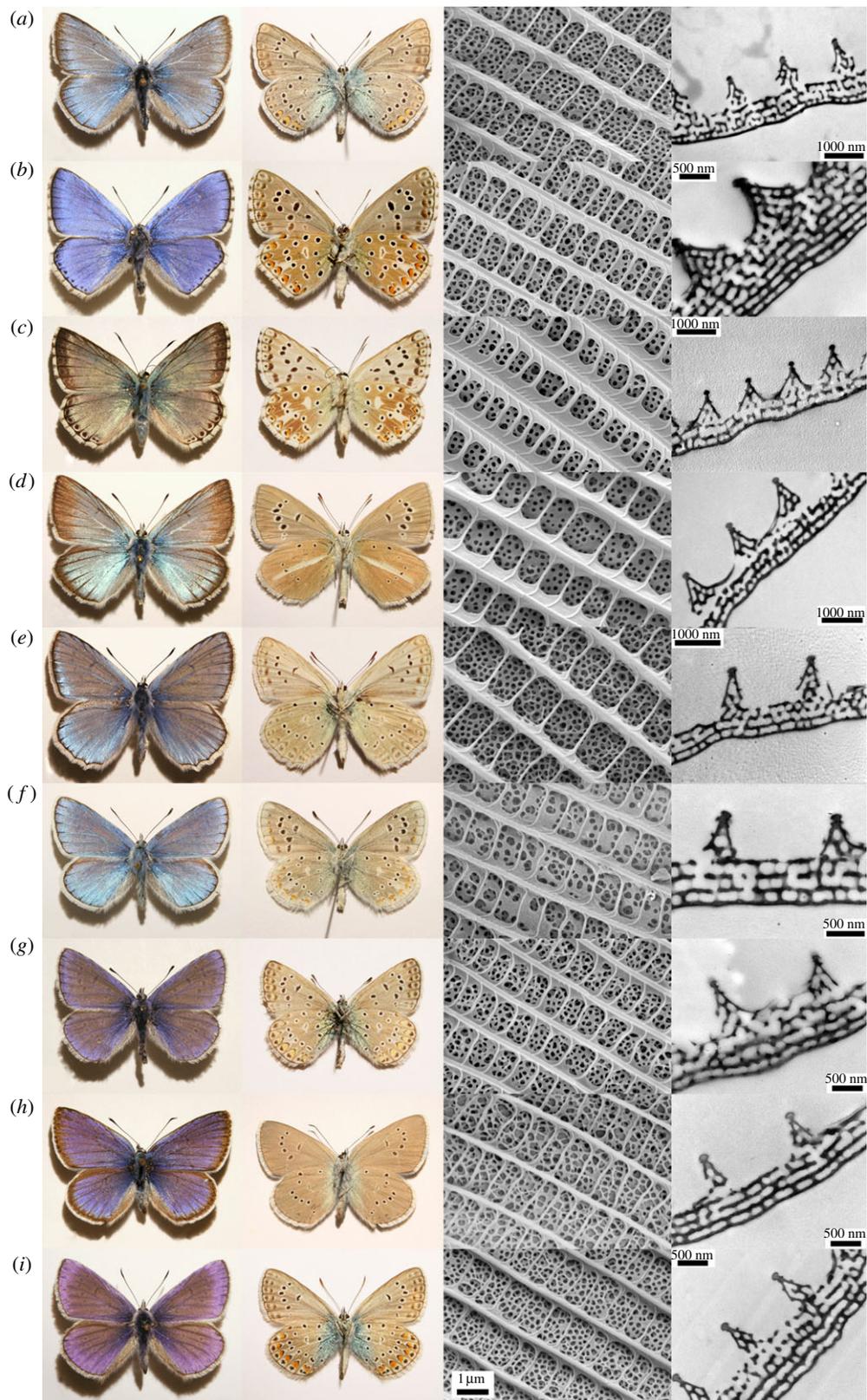
Figure 1. Optical dorsal and ventral images; SEM and TEM micrographs of the *Polyommatus* samples: (*a*) *P. amandus*, (*b*) *P. bellargus*, (*c*) *P. coridon*, (*d*) *P. damon*, (*e*) *P. daphnis*, (*f*) *P. dorylas*, (*g*) *P. icarus*, (*h*) *P. semiargus*, (*i*) *P. thersites*. Notice the complex pattern on the ventral sides.

belongs to the subtribe Polyommatina of the tribe Polyommatini and comprises approximately one-tenth of the relatively rich butterfly fauna typically found in Central Europe [23,30].

The local fauna sampled is situated geographically within the municipality border of Budapest, near Normafa (electronic supplementary material, figure S2), where the habitat is a mesophilous open grassland with high biodiversity existing on calciferous soil. All of the species tabulated (table 1) have been recorded at the site for more than a century. Currently, this is a unique habitat within the region, as one of the species

Table 1. Taxa investigated; listed in alphabetical order according to their subgeneric and species-group names. The right side lists the number of examined samples; all specimens are males; data for the specimens are listed in electronic supplementary material, table S1.

scientific name	Pc.
Polyommatus (Agrodiaetus) damon	10
Polyommatus (Cyaniris) semiargus	10
Polyommatus (Lysandra) bellargus	20
Polyommatus (Lysandra) coridon	10
Polyommatus (Meleageria) daphnis	10
Polyommatus (Neolysandra) amandus	10
Polyommatus (Plebicula) dorylas	20
Polyommatus (Polyommatus) icarus	10
Polyommatus (Polyommatus) theristes	10

(*Polyommatus damon*) occurs only here in the whole Carpathian Basin; thus, the fauna of the site has been strictly monitored every summer since 2000.

The chosen species represent a well-characterized monophyly in Polyommatina [31,32]. They have almost identical genital structures, androconia, wing venation and patterns and a very similar life history [33]. Certain taxa can be crossbred, resulting in hybrids that seldom occur in nature [34–36]. Within the monophyly, the species represent seven smaller monophyletic groups, which are labelled in table 1 by subgeneric names in parenthesis according to recent molecular studies [31,32,37]. Although these molecular results suggest a generic rank for most of the subgenera, for the sake of stressing the close relationship between the investigated species, we use *Polyommatus* in a 'supergenus' sense [38].

All of the males of the species we examined have blue dorsal wing surfaces of different hues. One species, *Polyommatus daphnis*, possesses a blue female phenotype. The males of the nine species and the female of *P. daphnis* have been investigated by reflectance spectroscopy using a recently developed instrument, the spectroboard [39]. The results of the *P. daphnis* blue female phenotype measurements are not included in this paper. The species *P. bellargus* and *Polyommatus icarus* are also known to have blue female morphs, but these do not occur at the site we sampled. All of the species examined display practically the same mating strategy: males patrol their habitats for mates and do not occupy any particular territory, as the closely related *Plebejus* (Polyommatina, Polyommatinae, Lycaenidae) do, which display highly sedentary behaviour [40–42].

All of the specimens used for the experimental studies carried out at the Research Institute for Technical Physics and Material Science of the Hungarian Academy of Sciences (HAS) originated from the scientifically curated butterfly collections of the Hungarian Natural History Museum (HNHM) and have been inventoried in the BioLep (for temporal and geographical data in HNHM) and BioPhot (for nanoarchitectural, optical and spectral data in HAS) databases. In our samples used for optical measurements and to characterize structural properties, every species was represented by at least 10 specimens collected from similar mesophilous habitats, such as Normafa, across Hungary. The optical and microstructural properties of this sample are representative of those of the investigated species found in the Pannonian region (electronic supplementary material, table S1). To construct histograms, we used the temporal occurrence data of 285 male specimens captured in Normafa or within a 20 km radius thereof, excluding variables caused by edaphic or microclimatic factors, which often strongly influence the ecology of butterfly populations (electronic supplementary material, table S2).

2.2. Experimental methods

The structure of the colour-generating cover scales was investigated by SEM and TEM. All samples investigated by means of SEM were prepared using the procedures described earlier [28]. Samples for SEM and TEM examination were cut from the right hindwings of the specimens. Small pieces of the wings were attached to stubs by double-sided carbon tape and were gold-sputtered to prevent charging. A high-resolution LEO 1540 XB scanning electron microscope was used for observation. A magnification of $50\,000\times$ was used to obtain all of the micrographs for ease of comparison. Cross sections of the wings used for TEM examination were prepared first by embedding the pieces of the wings in a special resin (EMbed 812). From sections measuring 70 nm in thickness, these samples were then cut by an ultramicrotome and transferred to copper grids. The samples were examined using a TECNAI 10 transmission electron microscope.

Optical spectroscopy was carried out using an Avantes 2048–2 fibre-optic spectrometer. Because a large number of fragile specimens were studied, to ensure reproducible, non-destructive and relatively rapid reflectance measurements, we used a dedicated home-built set-up [39], a so-called 'spectroboard'. In spectroscopic measurements and data evaluation, we followed the methodology described in an earlier paper [25]. All exemplars were measured using the 'spectroboard' over a fixed area of the right dorsal forewing. Wing surfaces were illuminated under normal incident light by a dual deuterium–halogen source; the reflected light was collected by the central core of the same optic-fibre bundle. The collected light was analysed over a wavelength range from 200 to 900 nm by the Avantes spectrophotometer. An Avantes white diffuse standard was used as a reference sample. To facilitate comparison, all curves were normalized to the highest peak in the blue range of the spectrum. To obtain the single-spectrum characteristics for a given butterfly species, the normalized spectra were averaged by species. This type of data reduction from a set of spectra to a single spectrum has the additional advantage of reducing the influence of minor individual variations arising from the different intervals of time elapsed between the emergence of the butterflies and their capture. During their life span, butterflies often lose a number of their scales because of exposure to destructive conditions. For the non-averaged spectra of *P. icarus*, see electronic supplementary material, figure S3.
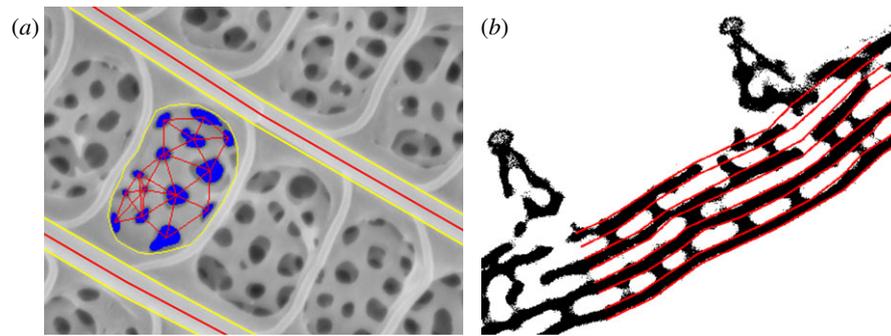
Figure 2. Using the Biophot Analyzer software for scanning and transmission electron micrograph feature extractions. (*a*) 'Pepper-pot' holes in a window are marked by the software according to user-chosen parameters (the marked regions turn blue), and then the software automatically determines the distance and shape-related values in a scanning electron micrograph; here, we can also read the widths and distances of ridges and cross-ribs. (*b*) On a processed (binarized) transmission electron micrograph image, layer thickness and distance are measured.

SEM and TEM examinations of the photonic nanoarchitectures revealed that the colours of all nine species are generated by the so-called 'pepper-pot' nanoarchitectures [29]. These materials possess a perforated multi-layer structure, as shown in fig. 6*e* in Biró & Vigneron [1]. Despite their similarity, the structures of the species must each present enough specificity to allow for the generation of the characteristic colours observed, which are perceived even by the naked eye (figure 1).

To extract the structural datasets from the SEM and TEM images, we used the Biophot Analyzer software [43; http://www.softadmin.ro/biophot/index.php]. This software, which is dedicated to the investigation of scale structure, allows for notations to be made on micrographs and automatically collects a large number of characteristic indices concerning scale structure.

The measured spectra and structural parameters were analysed using artificial neural network (ANN) software [44]. ANNs are computational models that are inspired by the structure and the functional aspects of biological neural networks. An ANN consists of an interconnected group of artificial neurons that work massively in parallel and that process information using a connectionist approach to computation [45]. Therefore, the ANN is an adaptive system; it has the capability to learn. Thus, it can be used in problems that cannot be formulated as algorithms, for example, data classification or pattern recognition.

An ANN is typically defined by three types of parameters [45]. First, an ANN is defined by the interconnection pattern between different layers of neurons. In our case, we used a standard three-layer network structure (input–hidden–output layers). The output layer contains nine output neurons for the nine species. The input layer contains a case-specific number of neurons (for structural or spectral investigations), one for each colour and structure identification parameter used. The number of neurons in the hidden layer was optimized independently for each of the two identification tasks. The second parameter is the activation function that converts a neuron's weighted input to its output activation. This is typically a nonlinear function; we used a tangent hyperbolic function in our network.

Table 2. The nine most significant structural parameters read from scanning electron micrographs and transmission electron micrographs. An array of nine data points for 225 measured 'windows' used as an input for the artificial neural network software.

average 'pepper-pot' filling factor
average 'pepper-pot' hole's deviation from the circle
average hole inner circle deviation from the hole diameter
　measured parallel to the ridges
average distance of the hole's centre of gravity
average number of hole neighbours
average maximum distance of first-neighbour holes
average width of the ridges in SEM micrographs
number of layers in TEM micrographs
average thickness of the layers in TEM micrographs

The third parameter is the learning process used to update the weights of the connections between the neurons. In this case, gradient-based back-propagation [46] was used, which is a supervised learning method for multi-layer networks.

3. RESULTS

3.1. Structural properties

As shown in the SEM and TEM micrographs of figure 1, all of the examined wing scales contain 'pepper-pot' structures. By visual inspection, one can perceive specific differences, but an exact quantitative comparison is hardly feasible. From the SEM images (identical 50 000 × magnification), one can extract the dimensional properties of the ridges and cross-ribs and of the perforated upper layer of the 'pepper-pot' structure. To gain in-depth information, TEM observations were made. Using the Biophot Analyzer software, we extracted a series of parameters representing the characteristic dimensions of the structures (electronic supplementary material, table S3). The basic units with which the structural analysis was carried out were the 'windows' of the 'pepper-pot' structure: the natural structural unit defined by two neighbouring ridges and cross-ribs. There are three groups of datasets: the distances and widths of ridges and cross-ribs, values describing the 'pepper-pot' structure (data

Table 3. Hit/miss table output of the artificial neural network (ANN) for the structural analysis. Correct answers are shown along the diagonal. The test was carried out on 225 windows, half of the total number of analysed windows (correct identifications: 91%).

result/expected	amandus	bellargus	coridon	damon	daphnis	dorylas	icarus	semiargus	thersites
amandus	14	0	0	2	0	0	0	2	0
bellargus	0	28	0	0	0	0	0	0	0
coridon	0	0	45	0	0	0	0	0	0
damon	1	0	0	29	0	1	0	1	0
daphnis	0	0	0	0	15	0	0	0	0
dorylas	0	0	0	0	0	13	1	0	0
icarus	2	0	0	0	0	0	41	1	0
semiargus	1	0	0	0	0	0	2	7	2
thersites	0	0	0	0	0	0	0	0	13

readable in 'windows') and layer thicknesses and distances derived from TEM images. For an example of data extraction using a 'window' from a TEM image (figure 2). After this procedure, we then obtained a total of 24 parameters. For the subsequent study carried out using the ANN software, nine parameters (table 2) seemed sufficient. After gathering data from the 450 'windows' of the scales of the nine species investigated, half of them were used for the teaching process of the ANN and the rest were used for testing. Hit results are shown in table 3: 205 windows were identified correctly (on table diagonal) from the 225 tests, yielding a 91 per cent accuracy.

3.2. Optical properties

The spectral conformity of conspecific exemplars is discussed in Bálint *et al.* [39]. The filtered normalized and averaged curves are presented in figure 3. To ease and automate spectral discrimination, the recognition marks must be extracted. To quantify the features of the spectra, we processed the curves following the algorithm shown in figure 4. From the three peaks × eight features, a total of 24 selected parameters for each spectrum were generated from the processing and were used in the ANN input array for the 110 exemplars (the features used were spectral position, intensity, area, full width at half maximum of the peaks, the position of base points on the left and right sides of the peaks and the left and right widths of the peak at half maximum). As shown in table 1, there are a minimum of 10 specimens for every species. Half of the total number of exemplars was used for network training; the remaining exemplars were used for testing. The results are presented in a manner similar to that of the previous section (table 4).

3.3. Temporal distribution

The temporal distribution of the butterflies can be described by the exact time of capture. To produce a larger dataset, in the HNHM collection, the time of capture for 285 exemplars was extracted from the records and represented in a histogram (figure 5). The larger number of exemplars is needed not only to detect the maximum occurrence but also to average the annual accidental differences caused by climate variations.
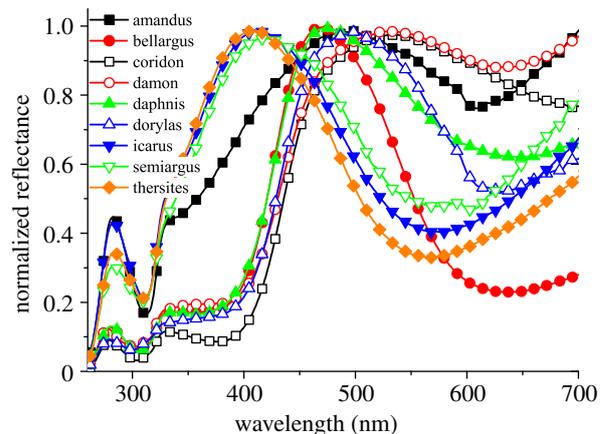

Figure 3. Averaged spectra of the nine investigated species showing the characteristic differences. To ease the comparison, they are normalized to the blue maxima, and a fast Fourier transform filter was applied for noise reduction.

3.4. Dedicated colour space of the investigated species

To facilitate the visual presentation of differences in wing colour, a graphical representation is useful. One method to compare colours is to plot the sample in the Commission Internationale de l'Eclairage (CIE) chromaticity diagram [47]. This is a two-dimensional representation of the reflectance spectrum hue that takes into account the human visible spectral range. This type of examination of the nine species was discussed earlier in Piszter *et al.* [25]. The studies concerning the Lepidoptera eye show the existence of four photoreceptors [48] for the investigated species. Compared with the human visible spectral range, this means that not only is there advanced sensitivity in the blue/UV range, but there is also a qualitative difference in colour differentiation. To gain a better approximation of how the butterflies see each other, based on the CIE tristimulus colour matching, we created a colour representation in three dimension instead of the standard chromaticity diagram (for details, see the electronic supplementary material). The resulting parameters are shown in a plot diagram (figure 6). Because the two-dimensional projection suitable for printing can render only a fraction of the three-dimensional information, a movie showing a
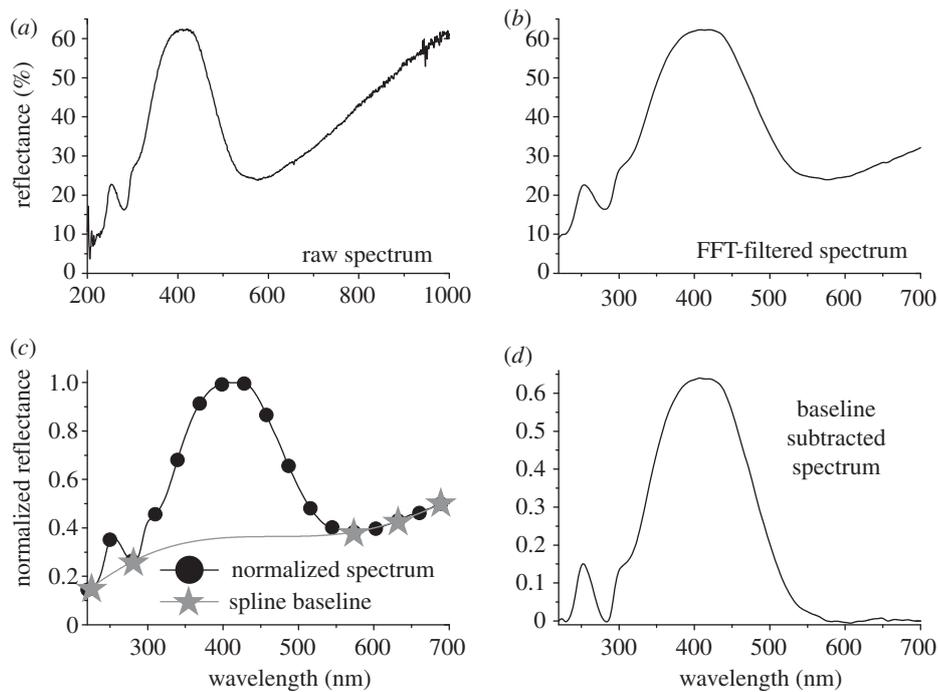
Figure 4. Pre-processing and feature extraction using individual spectra. (*a*) Raw data were filtered with a (*b*) fast Fourier transform filter after a cubic spline was fitted to (*c*) the minimum points and (*d*) subtracted to eliminate the non-structural component of the spectra. Then, with 'Origin 8' software, peak analysis was performed. Position, intensity, area, full width at half maximum of the peaks, the position of base points on the left and right side of the peaks and the left and right width of the peak at half maximum. These parameters were used as inputs for the artificial neural network software.

Table 4. Hit/miss table output of the ANN for the spectral analysis. Correct answers are shown along the diagonal. The test was carried out on 55 exemplars, half of the total number in the study (correct identifications: 96%).

result/expected	*amandus*	*bellargus*	*coridon*	*damon*	*daphnis*	*dorylas*	*icarus*	*semiargus*	*thersites*
amandus	5	0	0	0	0	0	0	0	0
bellargus	0	10	0	0	0	0	0	0	0
coridon	0	0	4	0	0	0	0	0	0
damon	0	0	1	5	0	0	0	0	0
daphnis	0	0	0	0	5	0	0	0	0
dorylas	0	0	0	0	0	10	0	0	0
icarus	0	0	0	0	0	0	5	0	1
semiargus	0	0	0	0	0	0	0	5	0
thersites	0	0	0	0	0	0	0	0	4

rotating three-dimensional plot is included in the electronic supplementary material (vid_2). As shown in figure 6 and in the movie in the electronic supplementary material, the nine species are better separated in the three-dimensional chromaticity diagram compared with the two-dimensional human chromaticity diagram used previously [25].

4. DISCUSSION

4.1. The importance of optical signal for blue butterfly males and females

The ventral wing surface, used as an important, human-invented taxonomic characteristic, is held still when an individual butterfly does not move (electronic supplementary material, figure S1). Hence, the males,

which generally patrol their habitats for prospective mates, must detect species-specific patterns against a background that is visually very complex (e.g. the random background of vegetation; see electronic supplementary material, video S3). Similarly, the females must detect males approaching at the high velocities of flight generated by the rapid beating of their wings (see electronic supplementary material, video S1). It is questionable whether the butterfly brain has enough processing power to recognize such fast motion (the time of a typical wing beat is of the order of 10–20 ms; see Imafuku & Ohtani [49] for related information on thecline lycaenid butterfly genus *Chrysozephyrus*) and store and analyse such complex patterns as those found on the ventral wing surfaces of the blues. Moreover, many of these patterns differ from each other only by minute details. The long-range recognition of conspecific
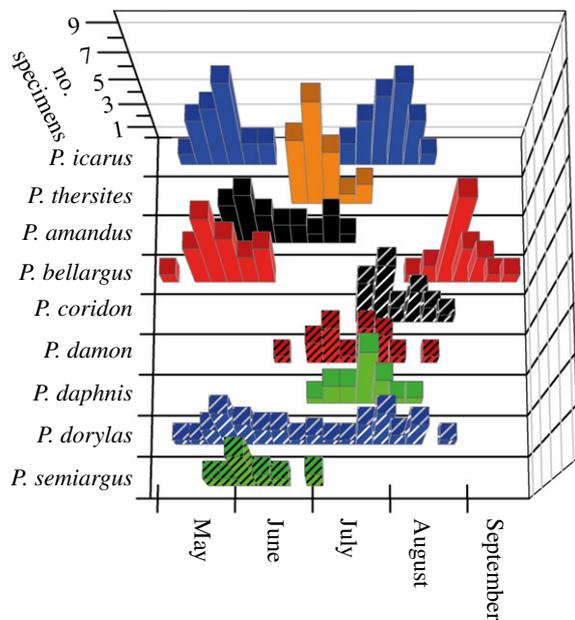
Figure 5. The temporal distribution of the investigated species in their habitat based on data of 285 male specimens. Notice the temporarily isolated and overlapping flight periods (for details, see §4).

individuals, for both males and females, may be advantageous in the case of fast-flying insects, as it can prevent numerous unsuccessful mating attempts.

Male polyommatine blue butterflies possess a complex system of androconia [50]; their role in courtship is only partly understood, but on the basis of published behavioural evidence, these androconia are not devices used to attract mates from long distances, as is the case for night flying moths, as shown by the classical experiments conducted by Fabre [51]. Field observations support the notion that male and female pheromones are used only when the mates are in tight physical contact [7]. It is worth briefly noting that in the case of the investigated butterfly species, it is not understood to what extent the genital structures alone may act as an effective barrier between species, as their genitalia are similar to the extent that the artificial cross-breeding of different taxa is possible [34,52]. Even if the genital structures act as sufficiently effective barriers, copulation attempts are usually the result of long periods of energy-intensive courtship [7]. Therefore, any signal, whether it is optical or chemical, that allows species discrimination before copulation must have great importance because it can prevent the wasting of energy. Indeed, it was experimentally demonstrated in the case of *Lycaeides argyrognomon* (Polyommatina, Polyommatinae, Lycaenidae) that before copulation, the chemical signals emitted by a male make the female display the receptive posture [7]. It has also been suggested that UV reflectivity increases the attractiveness of mate-searching males [9].

It is shown in the literature that if a male polyommatine blue butterfly is attracted by a female, the male flies towards her to start a courtship [53]. This contradicts the strong evidence that the male sex is far more conspicuous in every aspect (behaviourally, chemically and optically). If the male is more conspicuous in

appearance (generates a stronger optical signal than the female), more attractive in odour (the presence of androconia indicates that the male generates a stronger chemical signal than the female) and far more mobile, the following question arises: what is the primary and most important female signal? Another piece of evidence that prompts one to question the notion of female attractiveness is that the most conspicuous female pattern of the wing dorsal surface is the submarginal orange or red lunulation. According to recent experimental results for *P. icarus*, this pattern is invisible to the male sex, though polyommatine eyes seem to be perfectly tuned to the coloration displayed by male dorsal wing surfaces [48].

Our fieldwork and published results prove [42] that polyommatine females exhibit clearly different behaviour compared with males. Hatching females do not conspicuously display themselves when surrounded by vegetation but remain motionless close to the place where they hatched, and when an approaching male is observed, they conduct a short flight to catch the interest of the patrolling male. Although it has not been tested experimentally in the field, we formulated the hypothesis that this 'dance call' is displayed only for a male with a well-tuned colour. It is difficult to observe the 'dance call' in the field because usually females are encountered in copula or in nectaring or during ovipositing.

In subtropical–tropical forest habitats, polyommatine blues representing 'clades' other than *Polyommatus* exhibit an entirely different strategy to attract mates. The females, already in their pupal stage, emit strong odour signals to attract their mates for physical contact [54]. There is no such observation for polyommatine blues typical of temperate region grasslands. Polyommatine blue lycaenid caterpillars generally pupate and hatch in ant chambers [42], and when they leave their underground site, they climb up to a halm to complete the wing-stretching process. Immediately following this, the first dance and copulation takes place; therefore, virgin females are rarely encountered in the field. This is supported by the indirect evidence that captured female specimens in collections are almost always non-virgin ([34]; Zs. Bálint, personal observation).

4.2. Structural and optical properties

Although the ideal way of revealing the full three-dimensional structure of butterfly scales would be to use TEM tomography [55], the SEM and supplementary TEM images of the same area, if processed properly, are informative enough to collect a large number of characteristics. At first sight, the wing scales studied in this investigation seem to be very similar; however, they generate perceptible spectral differences, and the investigation of the structure by ANN demonstrates that the scales of the species studied in this work are characteristic of each species. Earlier, we showed in the case of *Albulina metallica* (Polyommatina, Polyommatinae, Lycaenidae) how the minor dimensional differences in the 'pepper-pot' structure induce very different aspects of the wing colour [56]. The most relevant factor in the determination of the spectral reflectance maxima is the average distance between the holes and the filling factor for the chitin. With
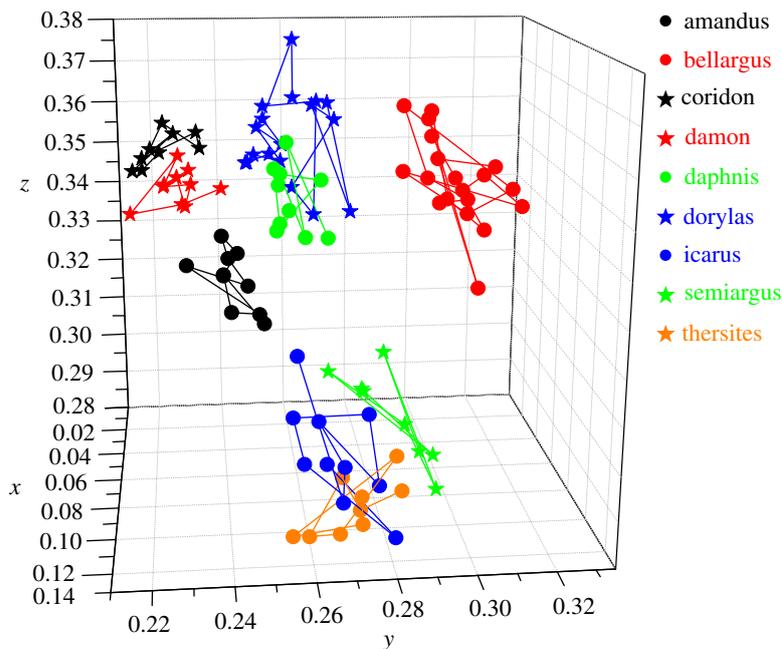
Figure 6. Individuals of nine species represented by colour *xyz* parameters (details in the electronic supplementary material). Notice the disjunct and incident domains for higher and smaller similarity of the colours (for details, see §4).

the Biophot Analyzer, we can measure a large number of submicron data from the structures from a top view (SEM) and in volume (TEM). For the discussed species, we found nine structural parameters that are important for the discrimination between the species (see the parameters in table 2). If a sufficiently large amount of data is available, one can set up an automated analyser to separate the images belonging to the species. The largest error in table 3 was obtained when *P. icarus* was identified as *Polyommatus thersites*. Their reflectance spectra (figure 3) are very similar to each other. In the ANN analysis of the spectral data, one of the two errors encountered occurred for these two species (table 4). The other was the identification of *Polyommatus coridon* as *Polyommatus damon*. This type of mistake can be attributed to the intensive cover-scale loss during the lifetime of the individual butterflies. The remaining ground-scales contain melanin, a typical brown pigment, which results in a relative increase in the reflectance over the 600–800 nm range.

The cross-correlated ANN investigation of structures and colours clearly shows that the species-specific colours are associated with species-specific structures. Taking into account the fact that relatively moderate alterations of structure observed by the naked eye in the SEM images (for example, parts (*a*) and (*b*) in figure 1 or the blue and green colours of *Albulina metallica* [56]) are responsible for significant colour differences, the characteristic structural patterns of the photonic nanoarchitectures must be encoded in the species' genetic material in a very precise and stable manner. It is highly likely that the individuals with the 'wrong' colour (and the wrong structure) are quickly eliminated in the mating competition. This suggests that it may be worth dedicating concentrated efforts to investigate the detailed structural and optical characterization of the nanoarchitectures occurring in

the scales of closely related species, which use their structural colours in sexual communication. Such an investigation, combined with detailed computer modelling, may offer new ideas regarding the design of novel bioinspired photonic nanoarchitectures.

The 110 exemplars were plotted in a three-dimensional colour diagram (figure 6), in which smaller distances between points indicate smaller differences in colour, as perceived by the butterflies. Taking the fourth visual pigment into account resulted in the dimensional extension of the colour space used by butterflies. Consequently, the partially overlapping regions observed previously in the two-dimensional (human) chromaticity diagram [25], which correspond to the nine butterfly species investigated, were well separated in three dimensions. As shown in the electronic supplementary material, movie, in some two-dimensional sections corresponding to certain rotation angles, several species show a high degree of overlap, despite the fact that they are well separated in three dimensions. The existence of the fourth visual pigment makes it possible to better discriminate between the differences in the UV–blue region, where most of the species-specific spectral characteristics are found. With the temporal distribution histogram and the colour representation diagram, we can show that butterflies with different hues of blue can coexist without disturbing one another's mating habits; meanwhile, species that exhibit nearly identical hues fly during different periods of the year.

4.3. The well-tuned blue colour of the blue males

According to their optical properties (figures 1 and 3), three groups of butterflies can be discerned at the site and can also be grouped together to a certain extent (figure 3) according to the three-dimensional colour representation diagram (figure 6): the violet

group (*icarus-semiargus-thersites*), the blue group (*bellargus-daphnis-dorylas*) and the greenish group (*amandus-coridon-damon*). The violet group is characterized by spectra with peaks that are narrower than those of the other species. The main maxima are almost overlapping; their discrimination by visual inspection according to colour only is a very difficult task (figure 1). Because of the presence of the secondary maxima in the range of 250 nm in the three-dimensional colour representation diagram, these species appear clearly separated (figure 6). The spectra in the blue group present a gradual broadening from *bellargus* to *dorylas* in such a way that the short-wavelength side of the main reflectance peak remains almost fixed, while the long-wavelength side is shifted to the right. A similar plateau is presented in all three spectra over a wavelength range from 325 to 400 nm; this region overlaps with the region in which the main reflectance peak of the violet group exhibits a clear shoulder. Near 250 nm, the secondary maxima of the blue species overlap. The spectra of the green group are characterized by an even more pronounced broadening towards longer wavelengths than that of the blue group. *Polyommatus amandus* is somewhat different from the other two members of the green group: it exhibits a very pronounced shoulder near 325 nm, almost overlapping with the shoulders of the violet group species, and it also exhibits a strong secondary maximum near 250 nm. The other two members of the green group exhibit spectra that are closer to those of the blue group in the short-wavelength region. Comparing the structures observed in the SEM images of figure 2, one may note that the pepper-pot structure of *P. amandus* has a higher filling factor compared with that of the violet species; meanwhile, the other two members of the green group, which also have structures with higher filling ratios than the species in the blue group, also exhibit a wider variation in the sizes of their perforations than the species in the blue group. Further work, combined with modelling, is required to gain deeper insight into the relationship between structural changes and their spectral effects. The fact that the ANN software was able to identify the nanostructures belonging to a certain species with a hit rate of 91 per cent, combined with the finding that the corresponding reflectance spectra are species-specific (ANN hit rate of 96%), suggests that there must be well-defined structural particularities that are responsible for the production of different hues of blue. This observation may not be as simple in the case of fully regular structures, where the periodicity of the structure—if the refractive index is held constant—primarily determines the position of the PBG. Nevertheless, it may be worth investing the effort to explore these dependencies because the quasi-ordered photonic nanoarchitectures occurring in butterfly scales very clearly demonstrate the wide range of possibilities for such nanocomposites.

4.4. Temporal distribution

In figure 5, the temporal distribution of all of the investigated species is shown; the histogram contains the data regarding a total of 285 exemplars. There are aggregations with one or two maxima, which indicate that *P. icarus*, *P. dorylas* and *P. bellargus* have a second

generation at the end of summer. Despite the large scatter in the sampling (counting randomly selected exemplars from 1930 to 2010), most of the histograms exhibit a well-defined maximum. For the blue wing surface to be a 'long-range' communicating signal suitable for species discrimination, a perceptible difference in colour is required. The four photoreceptors in the lycaenid butterfly eye support more detailed colour differentiation than the human eye. The presence of the additional blue visual pigment (curve 'u' in electronic supplementary material, figure S4) increases the capability of the butterflies to perceive spectral differences at wavelengths between 300 and 450 nm, exactly the range in which the smaller secondary maxima and the short-wavelength side of the main maximum are found. Based on the CIE colour representation, a parallel calculation was carried out for four wavelength-sensitive functions; the results are shown in figure 6. To the best of our knowledge, this is the first time that such a three-dimensional visual space has been used to investigate the colour discrimination capability of butterflies. This type of 'non-human' approach could prove to be useful in studying other butterflies as well [57]. However, it is worth noting that some butterfly species may have as many as eight types of visual receptors. In these cases, the construction of an adequate colour space may be a very complex task in n-dimensional geometry.

Regarding the temporal distribution of the flying periods of the investigated species, in the violet group, *P. icarus* and *P. thersites* are similar in colour, though *P. thersites* is inserted between the two generations of *P. icarus*. The small shift in *P. thersites* to the end of July is admissible because the members of this species will be old and will not perturb the mating of the second generation of *P. icarus*. In general, these species are quite well-separated temporally, which allows for better recognition, as their spectral differences are less significant (figure 3). The results show that there is an overlap between the flight periods of *P. icarus* and *P. semiargus*, but more thorough examination of the histograms reveals that the peak flight period of the first generation of *P. icarus* males occurs in mid-to-late May, when the first specimens of *P. semiargus* appear at the site; this latter species develops a long but single generation with a peak in mid-June. The species *P. thersites* starts to fly when the flight period of *P. semiargus* is almost over, when only aged *P. semiargus* specimens are present in the site.

In the blue group, there are two species with two generations: *P. bellargus* and *P. dorylas*. The generations of the first species produce the earliest and latest flight peaks in the habitat; although there is some overlap with the flight periods of *P. dorylas*, the spectral properties of the two species are clearly distinct. The flight period of the second generation of *P. dorylas* displays a clear overlap with that of the single-brooded *P. daphnis*. Although their spectra are sufficiently distinct to allow for species recognition, as has been demonstrated experimentally (see above), the isolation of the two species is supported by the unique phenomenon in the site that the *P. daphnis* females are always blue.

The species of the green group are single-brooded. The species *P. amandus* starts to fly long before the other two green species (*P. coridon* and *P. damon*). Although the *P. amandus* spectrum is quite distinctive, thereby

guaranteeing a species-specific signal, the male *P. amandus* individuals from the middle of June are generally worn and less reflective; consequently, they cannot be mistaken for the emerging fresh *P. damon* males. The spectrally very similar *P. coridon* and *P. damon* replace each other at the site. When *P. coridon* starts to swarm, the male individuals of *P. damon* are already worn and present in far smaller numbers; consequently, in the habitat, it is easy to distinguish the male *P. coridon* and *P. damon* individuals based on their dorsal wing colorations.

Beyond the groups discussed above, it is interesting to make a remark on the double-brooded species *P. icarus*, *P. dorylas* and *P. bellargus*. All of them exhibit a first-generation maximum in the middle or at the end of May, but their colour plots are very different from each other. This underlines the fact that these species have an immediately perceptible signal for discriminating between one another.

5. CONCLUSIONS

The complex structural and spectral investigation of the colours of nine closely related polyommatine species (living in the same habitat) with the males of all species possessing blue dorsal coloration on their wings revealed that the photonic nanoarchitectures responsible for the colour are species-specific, both structurally and spectrally. Using ANN software, the species were identified with an accuracy better than 90 per cent using either the structural data or the spectral data. Additionally, the investigation of the temporal distribution of the species throughout the year shows that the flight periods of the species with somewhat similar colours (as perceived by the human eye) are well separated. Furthermore, a colour representation diagram built in a manner analogous to that of the human CIE [47] diagram but taking into account the additional blue visual pigment of lycaenid butterflies yielded a much clearer distinction between the positions of the investigated species in the three-dimensional colour space of the butterflies when compared with previous calculations using the two-dimensional human colour space [25]. In short, taking into account the flying periods, the blue colours of the nine polyommatine species are well tuned to allow for safe mate/competitor recognition within the local butterfly fauna.

Detailed examination of the structure–colour correlation combined with modelling may reveal new bioinspired ways of designing artificial photonic nanoarchitectures with respect to the desired colour and hue.

REFERENCES

1 Biró, L. P. & Vigneron, J. P. 2011 Photonic nanoarchitectures in butterflies and beetles: valuable sources for bioinspiration. *Laser Photonics Rev.* **5**, 27–51. (doi:10.1002/lpor.200900018)

2 Ingram, A. L. & Parker, A. R. 2008 A review of the diversity and evolution of photonic structures in butterflies, incorporating the work of John Huxley (The Natural History Museum, London from 1961 to 1990). *Phil. Trans. R. Soc. B* **363**, 2465–2480. (doi:10.1098/rstb.2007.2258)

3 Prum, R. O., Quinn, T. & Torres, R. 2006 Anatomically diverse butterfly scales all produce structural colours by coherent scattering. *J. Exp. Biol.* **209**, 748–765. (doi:10.1242/jeb.02051)

4 Wilts, B. D., Leertouwer, H. L. & Stavenga, D. G. 2009 Imaging scatterometry and microspectrophotometry of lycaenid butterfly wing scales with perforated multilayers. *J. R. Soc. Interface* **6**, 185–192. (doi:10.1098/rsif.2008.0299.focus)

5 Kühn, A. 1955 *Vorlesungen über Entwicklungsphysiologie.* Berlin, Germany: Springer-Verlag.

6 Ghiradella, H. T. & Butler, M. W. 2009 Many variations on a few themes: a broader look at development of iridescent scales (and feathers). *J. R. Soc. Interface* **6**, 243–251. (doi:10.1098/rsif.2008.0372.focus)

7 Lundgren, L. & Bergström, G. 1975 Wing scents and scent-released phases in the courtship behavior of *Lycaeides argyrognomon* (Lepidoptera: Lycaenidae). *J. Chem. Ecol.* **1**, 399–412.

8 Lundgren, L. 1977 Role of intra and interspecific male—male interactions in *Polyommatus icarus* Rott. and some other species of blues (Lycaenidae). *J. Res. Lepid.* **16**, 249–264.

9 Pellmyr, O. 1983 Plebeian courtship revisited: studies on the female-produced male behavior-eliciting signals in *Lycaeides idas* courtship (Lycaenidae). *J. Res. Lepid.* **21**, 147–157.

10 Lukhtanov, V. A., Kandul, N. P., Plotkin, J. B., Dantchenko, A. V., Haig, D. & Pierce, N. E. 2005 Reinforcement of pre-zygotic isolation and karyotype evolution in *Agrodiaetus* butterflies. *Nature* **436**, 385–389. (doi:10.1038/nature03704)

11 Biró, L. P. *et al.* 2003 Role of photonic-crystal-type structures in the thermal regulation of a lycaenid butterfly sister species pair. *Phys. Rev. E* **67**, 021907–021907. (doi:10.1103/PhysRevE.67.021907)

12 Yablonovitch, E. 1987 Inhibited spontaneous emission in solid-state physics and electronics. *Phys. Rev. Lett.* **58**, 2059–2062. (doi:10.1103/PhysRevLett.58.2059)

13 John, S. 1987 Strong localization of photons in certain disordered dielectric supperlattices. *Phys. Rev. Lett.* **58**, 2486–2489. (doi:10.1103/PhysRevLett.58.2486)

14 Joannopoulos, J. D., Meade, R. & Winn, D. J. N. 1995 *Photonic crystals: molding the flow of light.* Princeton, NJ: Princeton University Press.

15 Kristensen, N. P. 2003 *Lepidoptera, moths and butterflies: morphology, physiology, and development.* Walter De Gruyter Inc.

16 Nijhout, H. F. 1991 *The development and evolution of butterfly wing patterns.* Washington, D.C.: Smithsonian Institution Press.

17 Parker, A. R. 1998 Colour in Burgess Shale animals and the effect of light on evolution in the Cambrian. *Proc. R. Soc. Lond. B* **265**, 967–972. (doi:10.1098/rspb.1998.0385)

18 Vukusic, P., Sambles, J. R., Lawrence, C. R. & Wootton, R. J. 1999 Quantified interference and diffraction in single morpho butterfly scales. *Proc. R. Soc. Lond. B* **266**, 1403–1411. (doi:10.1098/rspb.1999.0794)

19 Berthier, S. 2003 *Iridescences: les Couleurs Physiques des Insects.* Paris, France: Springer.

20 Srinivasarao, M. 1999 Nano-optics in the biological world: beetles, butterflies, birds, and moths. *Chem. Rev.* **99**, 1935–1961. (doi:10.1021/cr970080y)

21 Kinoshita, S. 2008 *Structural colors in the realm of nature.* New Jersey, NJ: World Scientific.

22 Arsenault, A. C., Puzzo, D. P., Manners, I. & Ozin, G. A. 2007 Photonic-crystal full-colour displays. *Nat. Photonics* **1**, 468–472. (doi:10.1038/nphoton.2007.140)

23 Bálint, Zs., Horváth, Z. E., Kertész, K., Vértesy, Z. & Biró, L. P. 2007 Observations on scale structures and spectroscopic properties of *Polyommatus* lycaenid butterflies (Lepidoptera: Lycaenidae). *Ann. Hist. Nat. Mus. Natl Hung.* **99**, 115–127.

24 Bálint, Zs., Boyer, P., Kertész, K. & Biró, L. P. 2008 Observations on the spectral reflectances of certain high Andean *Penaincisalia* and *Thecloxurina*, with the description of a new species (Lepidoptera: Lycaenidae: Eumaeini). *J. Nat. Hist.* **42**, 1793–1804. (doi:10.1080/00222930802097675)

25 Piszter, G., Kertész, K., Vértesy, Z., Bálint, Zs. & Biró, L. P. 2010 Color based discrimination of chitin–air nanocomposites in butterfly scales and their role in conspecific recognition. *Anal. Methods* **3**, 78–83. (doi:10.1039/c0ay00410c)

26 Biró, L. P., Kertész, K., Vértesy, Z., Márk, G. I., Bálint, Zs., Lousse, V. & Vigneron, J. P. 2008 Living photonic crystals: butterfly scales—nanostructure and optical properties. *Mater. Sci. Eng. C* **27**, 941–946. (doi:10.1016/j.msec.2006.09.043)

27 Bálint, Zs., Vértesy, Z. & Biró, L. P. 2005 Microstructures and nanostructures of high Andean *Penaincisalia* lycaenid butterfly scales (Lepiodptera: Lycaenidae): descriptions and interpretations. *J. Nat. Hist.* **39**, 2935–2952. (doi:10.1080/00222930500140629)

28 Kertész, K., Bálint, Zs., Vértesy, Z., Márk, G. I., Lousse, V., Vigneron, J. P., Rassart, M. & Biró, L. P. 2006 Gleaming and dull surface textures from photonic-crystal-type nanostructures in the butterfly *Cyanophrys remus*. *Phys. Rev. E* **74**, 021922. (doi:10.1103/PhysRevE.74.021922)

29 Tilley, R. J. D. & Eliot, J. N. 2002 Scale microstructure and its phylogenetic implications in lycaenid butterflies (Lepidoptera, Lycaenidae). *Trans. lepid. Soc. Jpn* **53**, 153–180.

30 Bálint, Zs. 2003 In *Prime butterfly areas in Europe: priority sites for conservation* (eds C. A. M. van Sway & M. S. Warren), pp. 289–317. The Netherlands: Ministry of Agriculture, Nature Management and Fisheries.

31 Wiemers, M., Stradomsky, B. V. & Vodolazhsky, D. I. 2010 A molecular phylogeny of *Polyommatus* s. str. and *Plebicula* based on mitochondrial COI and nuclear ITS2 sequences (Lepidoptera: Lycaenidae). *Eur. J. Entomol.* **107**, 325–336.

32 Wiemers, M., Keller, A. & Wolf, M. 2009 ITS2 secondary structure improves phylogeny estimation in a radiation of blue butterflies of the subgenus *Agrodiaetus* (Lepidoptera: Lycaenidae: Polyommatus). *BMC Evol. Biol.* **9**, 300. (doi:10.1186/1471-2148-9-300)

33 Szabó, R. 1956 Magyarország Lycaenidái. (The lycaenids of Hungary). *Folia Entomol. Hung. Series Nova* **9**, 236–362.

34 Schurian, K. G. 1989 Revision der Lysandra-Gruppe des Genus Polyommatus Latr. (Lepidoptera: Lycaenidae). *Neue Ent. Nachr.* **24**, 1–181.

35 Schurian, K. G. 1989 Bemerkungen zu Lysandra cormion Nabokov, 1941 (Lepidoptera: Lycaenidae). *Nachr. Ent. Ver. Apollo (NF)* **10**, 183–192.

36 Schurian, K. G. 1991 Nachtrag zu den 'Bemerkungen zu 'Lysandra cormion' (Lepidoptera: Lycaenidae). *Nachr. Ent. Ver. Apollo (NF)* **12**, 193–195.

37 Vila, R. *et al.* 2011 Phylogeny and paleoecology of *Polyommatus* blue butterflies show Beringia was a climate-regulated gateway to the New World. *Proc. R. Soc. Lond. B* **278**, 1–8. (doi:10.1098/rspb.2010.2213)

38 Tshikolovets, V. 2011 *Butterflies of Europe and the Mediterranean area.* Pardubice, Czech Republic: Tshikolovets Publications.

39 Bálint, Zs., Wojtusiak, J., Piszter, G., Kertész, K. & Biró, L. P. 2010 Spectroboard: an instrument for measuring spectral characteristics of butterfly wings—a new tool for taxonomists. *Genus* **21**, 163–168.

40 Ravescroft, N. O. M. 1990 The ecology and conservation of the silver-studded blue butterfly *Plebejus argus* L. on the sandlings of East Anglia, England. *Biol. Conserv.* **53**, 21–36. (doi:10.1016/0006-3207(90)90060-3)

41 Bálint, Zs. & Fiedler, K. 1993 *Plebeius sephirus* (Frivaldszky, 1835) in Pannonia, with special reference to its status and ecology in Hungary. *Oedippus* **4**, 1–24.

42 Thomas, J. & Lewington, R. 2010 *The butterflies of Britain and Ireland.* Gillingham, UK: British Wildlife Publishing Ltd.

43 Kertész, K. *et al.* 2008 Photonic band gap materials in butterfly scales: a possible source of 'blueprints'. *Mater. Sci. Eng. B* **149**, 259–265. (doi:10.1016/j.mseb.2007.10.013)

44 Gurney, K. 1997 *An introduction to neural networks.* London, UK: UCL Press. (Taylor & Francis group).

45 Kriesel, D. 2007 *A brief introduction to neural networks.* See http://www.dkriesel.com

46 Bryson, A. E. & Ho, Y.-C. 1969 *Applied optimal control: optimization, estimation, and control.* Waltham, MA: Blaisdell.

47 Ohno, Y. 2000 CIE Fundamentals for color measurements. In *Int. Conf. on Digital Printing Technologies, 15–20 October 2000, Vancouver, Canada,* pp. 540–545. Springfield, VA: Society for Imaging Science and Technology.

48 Sison-Mangus, M. P., Briscoe1, A. D., Zaccardi, G., Knüttel, H. & Kelber, A. 2008 The lycaenid butterfly *Polyommatus icarus* uses a duplicated blue opsin to see green. *J. Exp. Biol.* **211**, 361–369. (doi:10.1242/jeb.012617)

49 Imafuku, M. & Ohtani, T. 2006 Analysis of coordinated circling and linear flight of a lycaenid butterfly species. *Naturwissenschaften* **93**, 131–135. (doi:10.1007/s00114-005-0074-x)

50 Eliot, J. N. 1973 The higher classification of the Lycaenidae (Lepidoptera): a tentative arrangement. *Bull. Br. Mus. Nat. Hist. Entomol.* **28**, 371–505.

51 Fabre, J.-H. 1979 *A rovarok környezete és viselkedése. (The environment and behaviour of insects).* Bukarest, Romania: Kriterion.

52 Gil-T., F. 2007 A natural hybrid between *Polyommatus bellargus* (Rottemburg, 1775) x *P. albicans* (Herrich-Schäffer, 1852) and notes about a probable hybrid of *P. punctifera* (Oberthür, 18760) x *P. albicans* (Lpeiodptera: Lycaenidae). *Nachr. ent. Ver. Apollo (NF)* **28**, 11–13.

53 Burghardt, F., Knüttel, H., Becker, M. & Fiedler, K. 2000 Flavonoid wing pigments increase attractiveness of female common blue (*Polyommatus icarus*) butterflies to mate-searching males. *Naturwissenschaften* **87**, 304–307. (doi:10.1007/s001140050726)

54 Elgar, M. A. & Pierce, N. A. 1988 Mating success and fecundity in an ant-tended lycaenid butterfly. In *Reproductive success: studies of selection and adaptation in contrasting breeding systems* (ed. T. H. Clutton-Brock), pp. 59–75. Chicago, IL: Chicago University Press.

55 Argyros, A., Manos, S., Large, M. C. J., McKenzie, D. R., Cox, G. C. & Dwarte, D. M. 2002 Electron tomography and computer visualisation of a three-dimensional 'photonic' crystal in a butterfly wing-scale. *Micron* **33**, 483–487. (doi:10.1016/S0968-4328(01)00044-0)

56 Márk, G. I., Vértesy, Z., Kertész, K., Bálint, Zs. & Biró, L. P. 2009 Order-disorder effects in structure and color relation of photonic-crystal-type nanostructures in butterfly wing scales. *Phys. Rev. E* **80**, 051903. (doi:10.1103/PhysRevE.80.051903)

57 Kelber, A. & Osorio, D. 2010 From spectral information to animal colour vision: experiments and concepts. *Proc. R. Soc. Lond. B* **277**, 1617–1625. (doi:10.1098/rspb.2009.2118)